OPEN ACCESS
IOP Publishing

Measurement Science and Technology

Meas. Sci. Technol. **35** (2024) 025027 (12pp)

https://doi.org/10.1088/1361-6501/acfe30

A numerical study of the anisotropic distribution of γ-ray emission from oriented ^{129m,131m,133m}Xe

Karolina Kulesz[1,2], Robin Yoël Engel[1,3], Renaud Blaise Jolivet[4,*] and Magdalena Kowalska[1,2,*]

[1] CERN, Espl. des Particules 1, Meyrin 1211, Switzerland
[2] University of Geneva, Quai Ernest-Ansermet 24, Geneva 1205, Switzerland
[3] Carl von Ossietzky Universität Oldenburg, Ammerländer Heerstr. 114-118, 26129 Oldenburg, Germany
[4] Maastricht Centre for Systems Biology (MaCSBio), Maastricht University, Paul-Henri Spaaklaan 1, Maastricht 6229 EN, The Netherlands

E-mail: r.jolivet@maastrichtuniversity.nl and kowalska@cern.ch

Received 25 May 2023, revised 19 September 2023
Accepted for publication 28 September 2023
Published 20 November 2023

Abstract

Spin-polarized radioactive nuclei emit radioactive decay products in an anisotropic manner that is characteristic of their degree of nuclear orientation. This property can be utilized for nuclear magnetic resonance spectroscopy and imaging. In this manuscript, we present Python and MATLAB numerical simulations that investigate the angular distribution and measurable asymmetry of γ-ray emission from spin-oriented nuclei of the metastable isotopes ^{129m,131m,133m}Xe. We examine several cases that represent different degrees of spin alignment and detection geometries. The results of our simulations provide a benchmark for experiments that use γ-decay anisotropy, such as the GAMMA-MRI project, which aims to develop a novel medical-imaging technique combining the strengths of magnetic resonance and nuclear medicine imaging.

Keywords: nuclear spin orientation, nuclear alignment, γ-ray emission anisotropy, spin temperature, hyperpolarization

1. Introduction

Over the past few decades, several authors have presented detailed discussions on the topic of nuclear spin orientation[5] and the resulting angular correlations and angular distribution of nuclear radiation [2–7]. Some of these studies were specifically focused on γ-emitting nuclei. In nuclear-structure research, γ-emitting nuclei were utilized to determine the spins and parities of excited states in nuclei [2, 3], or to measure magnetic moments of unstable nuclei through γ-detected nuclear magnetic resonance (gamma-NMR) [8, 9]. More recently, γ-ray-detected magnetic resonance imaging

* Authors to whom any correspondence should be addressed.

[5] Note that we use the term 'orientation' as the most general form of uneven distribution of spin population, encompassing polarization (or vector polarization) and alignment (tensor polarization) [1]. In other communities the terms are interchanged, namely polarization is more general than orientation and alignment.

(gamma-MRI) has even been proposed as a potential medical diagnostic application [10], which is now the focus of the European GAMMA-MRI project, as described at https://gamma-mri.eu.

The GAMMA-MRI project aims to combine the principles of nuclear spin manipulation used in magnetic resonance imaging (MRI), with the highly efficient detection of γ-rays used in single photon emission tomography. Specifically, the project relies on: (1) external spin orientation of unstable γ-emitting nuclei inside a magnetic field; (2) measurement of the asymmetry in the angular distribution of the emitted γ radiation, which depends on the degree of orientation; and (3) application of MRI sequences to manipulate the spins in a selected volume of space and thus to modify the angular distribution of radiation for image reconstruction [11].

Here, we present analytical calculations and numerical simulations of the anisotropic distribution of γ-rays emitted by metastable xenon isotopes $^{129\mathrm{m},131\mathrm{m},133\mathrm{m}}$Xe, which are feasible candidates for the GAMMA-MRI technique. The calculations are based on the additional assumption that the spin orientation can be described by the so-called *spin temperature*. Our results aim to support the optimization of spin orientation and detector asymmetry in the GAMMA-MRI project.

Conventional MRI works by manipulating the net magnetization of protons, i.e. the population difference between the spin-up and spin-down levels. The Boltzmann distribution predicts that in the static magnetic field of a typical MRI scanner with a field strength of $\mathbf{B} = 1.4\,\mathrm{T}$ the relative difference in these two populations is small, on the order of 10^{-5}. Therefore, conventional MRI is heavily dependent on the abundance of hydrogen atoms in biological tissues to achieve feasible signals, and necessitates strong magnetic fields.

However, it is possible to engineer *ex situ* a larger difference between spin populations, by means other than increasing the magnetic field. These approaches are known as hyperpolarization (HP). One such technique is spin–exchange optical pumping (SEOP), which has been extensively described for non-radioactive noble gases by Walker and Happer [12], and others [13, 14]. SEOP uses circularly polarized light from a laser to polarize alkali atoms in a gas phase (rubidium or cesium), within a glass cell placed in a weak magnetic field (several mT). A pair of Helmholtz coils generates a homogeneous magnetic field in the cell's region, providing an orientation axis for the polarized atoms. During binary collisions and three-body interactions in the formation of van der Waals molecules with nitrogen, the hyperfine interaction between the alkali-metal electron and the noble-gas nucleus makes them partially exchange angular momentum. Repeated interactions lead to a build-up of nuclear spin orientation of mXe up to several tens of percent. The build-up of nuclear orientation can be monitored conveniently by continuous or pulsed NMR excitations.

In comparison to stable He and Xe, SEOP of radioactive noble gases (namely Xe) was performed only by Calaprice *et al* [8], and much more recently by Zheng *et al* [10]. In the above cases, the SEOP process was followed by NMR or MRI rf pulse sequences, respectively.

In the GAMMA-MRI approach, in addition to exploiting HP, one utilizes a different detection scheme compared to conventional MRI. Instead of detecting the weak electromagnetic signal induced by rotating spins using inductive pickup coils, one measures the anisotropic emission of γ-rays, as demonstrated in [8, 10]. This method offers an advantage over conventional MRI as, unlike radio-frequency (rf) photons, even individual γ-ray photons can be easily discerned and detected with high probability. In principle, this detection scheme allows us to reach excellent sensitivity to small amounts of tracer nuclei in the sample volume.

The paper is organized as follows: in section 2, we summarize the mathematical description of nuclear orientation and γ decay characteristics, and lay out the idealized measurement geometry that was used for the computations presented in the section 3, and discussed in section 4. Here, a number of test cases are introduced to illustrate the effect of various parameters on the detected asymmetry. Specifically, we consider the impact of polarization and alignment, the relevance of higher-order multipolar emission contributions, and differences in the experimental geometry of the sample and detector. We conclude our findings with respect to the GAMMA-MRI project in section 4.

2. Model assumptions

2.1. Description of the model

In the simulations presented here, we consider the instantaneous nuclear alignment of radioactive xenon nuclei and the resulting angular distribution of the emitted γ radiation. Notably, we do not include considerations on the process of SEOP, such as the achievable degree of Rb atom polarization, the rates of spin orientation transfer from rubidium atoms to xenon nuclei, as well as losses of xenon orientation over time. This has been treated in detail elsewhere [12, 15].

Spin temperature T_s and spin temperature parameter β are useful parameters to describe an ensemble of identical interacting spins that have been brought out of thermal equilibrium and have not yet returned back to it (e.g. mXe after spin orientation via spin exchange optical pumping) [16]. In that case, the population p_m of the magnetic sublevels of the spins is characterized by a Boltzmann distribution [16] with $p_m \propto e^{-m/(kT_s)}$ (k is the Boltzmann constant) and therefore can be described with only one parameter T_s, analogous to a 'real' temperature for a system in thermal equilibrium. The dimensionless β which we use in the manuscript is defined as $\beta = -1/(kT_s)$.

Three isomers (i.e. long-lived excited nuclear states) are of interest for the GAMMA-MRI project: $^{129\mathrm{m}}$Xe, $^{131\mathrm{m}}$Xe, and $^{133\mathrm{m}}$Xe, to which we refer further as mXe. All three have spins $I = {}^{11}\!/_{2}$ and decay via a pure $M4$ γ-ray transition to $I = {}^{3}\!/_{2}$ state, which is either the ground state or first excited state. Their decay schemes are shown in figure 1 [17–19].

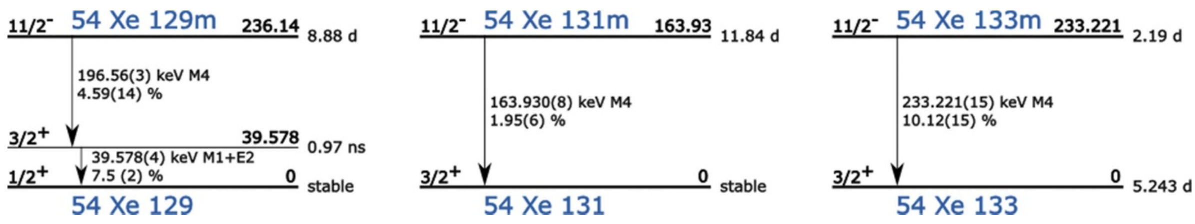

Figure 1. Radioactive decay schemes of the isomers ^{129m}Xe, ^{131m}Xe and ^{133m}Xe drawn using reference [17–19].

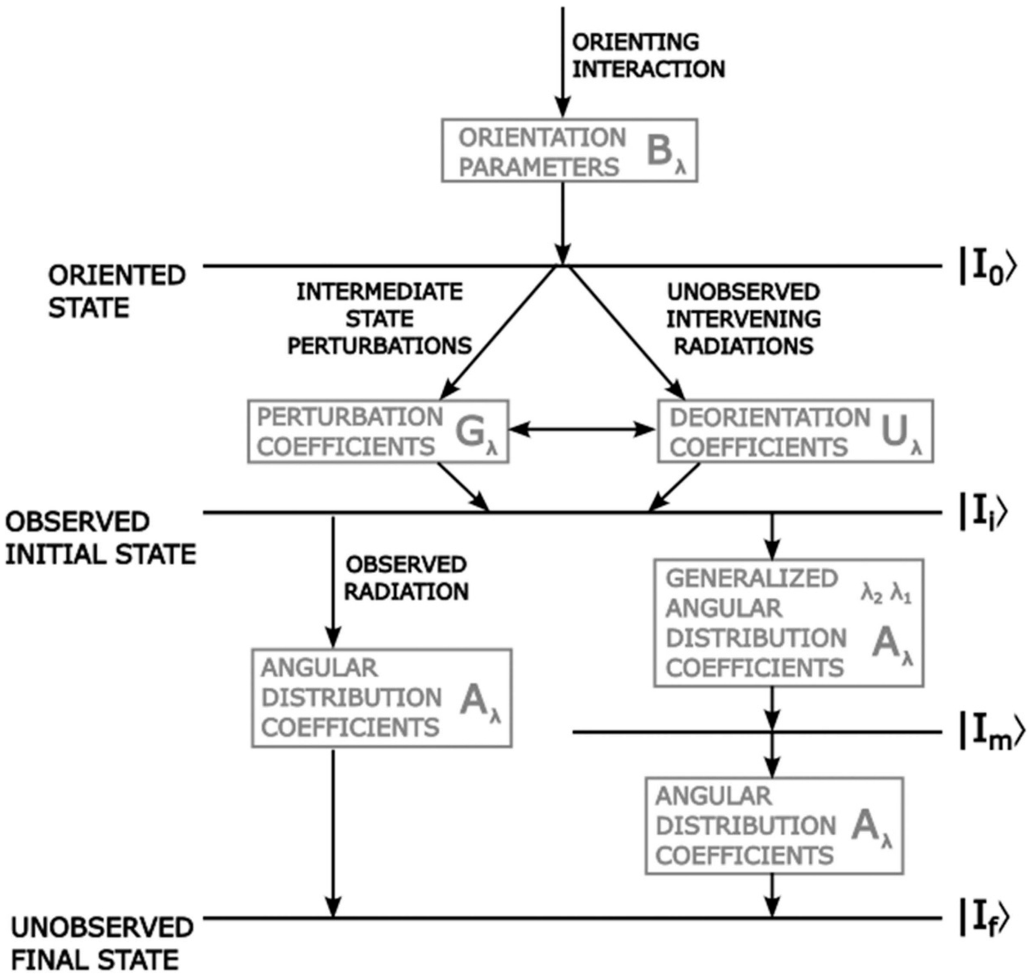

Figure 2. Schematic diagram showing the nuclear states and parameters involved in the parametrization of angular distribution measurements from oriented nuclei. Drawing based on [2], chapter 2: *Nuclear Orientation Formalism*.

In the following, we describe the angular distribution of γ radiation for these nuclear spins and the type of γ radiation.

2.2. Anisotropic distribution of γ radiation from oriented nuclei

In order to describe the angular distribution $W(\theta)$ for a certain type of decay radiation emitted by an ensemble of oriented nuclei (at angle θ) to the quantization axis), several coefficients have to be known. Figure 2 illustrates the nature of these coefficients.

I_0 is the spin of the original oriented state, the parent state of the radioactive decay, or the initial state of a nuclear reaction. I_f is the final state, and I_m the intermediate state, for cases with two or more intermediate radiations. B_λ are the nuclear orientation parameters describing the initial oriented state. λ is connected to the type of radiation and the multipolarity L of the radiation emitted between the oriented I_0 state and the final state I_f. For example, for β emission only odd λ's are relevant, compared to even λ's for γ-ray emission. The maximum λ is given by the multipolarity L of the emitted radiation $\lambda_{\max} = 2L$ (with $L = 2$ for dipole transitions, $L = 4$ for quadrupole transitions, etc). For $M4$ γ-ray transitions studied here, $L = 4$ and thus $\lambda \in \{2, 4, 6, 8\}$.

In the most general case, the $B_\lambda(I)$ are calculated using statistical tensors in the density matrix formalism [20]. In the particular case when the orienting interaction has an axis of symmetry (such as is the case in here), the diagonal elements of the density matrix are used as population parameters p_m, with $m' = m$, and the equation for $B_\lambda(I = I_0)$ simplifies to:

$$B_\lambda(I_0) = \sqrt{(2\lambda+1)(2I_0+1)} \sum_m (-1)^{I_0+m} \times \begin{pmatrix} I_i & \lambda & I_i \\ -m & 0 & m \end{pmatrix} p_m, \tag{1}$$

where the weights are given by the Wigner 3-j symbol.

U_λ are the orientation coefficients that depend on the properties of the intervening intermediate radiations. U_λ determines the orientation of I_i by modifying the orientation of I_0. If there is no intervening radiation, I_i is identical to I_0, and U_λ are equal to 1. This is the case for the $^{11}/_2$ state of metastable xenon.

G_λ is the perturbation coefficients describing the direct interaction of the electromagnetic moments of a long-lived intermediate state I_i with the nuclear environment (if such long-lived states exist). Coefficients G_λ refer to the same phenomenon as relaxation in magnetic resonance terms. In the numerical simulations, they were assumed to be 1, and thus the initial state was the same as the originally oriented state, and there were no time-varying relaxation processes. Finally, A_λ are the angular distribution coefficients that depend on the radiation type and transition multipolarity for the observed radiation. In the case of multiple radiations, where it might be advantageous to measure two emissions in coincidence, we would differentiate between A_{λ_1} and A_{λ_2} (generalized angular distribution coefficients in figure 2). In our case, where we have a single transition, i.e. for $I_i \to I_f$ transition, A_λ is:

$$A_\lambda = \frac{1}{1+\sigma^2}\left[F_\lambda(L,L',I_f,I_i) + 2\sigma F_\lambda(L,L',I_f,I_i) + \sigma^2 F_\lambda(L,L',I_f,I_i)\right], \tag{2}$$

where L and L' are the previously-mentioned angular momenta of the γ radiation and $L' = 0$, as the mixing ratio $\sigma = 0$ for the pure multipole transitions. $F_\lambda(L,L',I_f,I_i)$ are multipole functions with Wigner 3-j symbol and 6-j symbol. $F_\lambda(L,L',I_f,I_i)$ are tabulated, e.g. in [2, 21]:

$$\begin{aligned} &F_\lambda(L,L',I_f,I_i) \\ &= (-1)^{I_f+I_i+1}\sqrt{(2\lambda+1)(2L+1)(2L'+1)(2I_i+1)} \\ &\times \begin{pmatrix} L & L' & \lambda \\ 1 & -1 & 0 \end{pmatrix} \begin{Bmatrix} L & L' & \lambda \\ I_i & I_i & I_f \end{Bmatrix}. \end{aligned} \tag{3}$$

For the case studied here ($\sigma = 0$), coefficients $A_\lambda = F_\lambda(L = 4, L' = 0, I_f, I_0)$.

For the axially symmetric oriented states we discuss here, the general expression for the normalized directional distribution of γ-ray transition given in [2] (chapter 2.6) can be simplified to a form of a multiple expansion:

$$W(\theta) = 1 + \sum_{\lambda\ even} B_\lambda U_\lambda G_\lambda A_\lambda Q_\lambda P_\lambda(\cos\theta), \tag{4}$$

with the solid angle correction factor Q_λ that compensates for the finite solid angles subtended by the source and the detector. If we assume that the source and the detector are each geometrical points, and thus that the direction of the radiation emission can be uniquely specified, then $Q_\lambda = 1$. Finally, $P_\lambda(\theta)$ is the Legendre polynomial of order λ, and θ is the azimuthal angle between radiation and z-axis, around which the radiation is axially symmetric. Rodrigues' formula gives a compact expression for the Legendre polynomials, namely: $P_n(x) = \frac{1}{2^n n!}\frac{\mathrm{d}^n}{\mathrm{d}x^n}(x^2-1)^n$.

In the simulations, we assume a negligible size for the source and detectors, and no intervening intermediate radiations for the $^{11}/_2$ state. Thus, we take U_{λ_j}, G_λ, and Q_λ as each equal to 1. Coefficients A_λ and B_{λ_j} are explicitly calculated and given as an output of the simulations, and so is the resulting angular distribution $W(\theta)$ plotted as a two-dimensional figure.

2.3. Evaluating spin orientation

Nuclear orientation can be described using $B_\lambda(I_0)$ parameters up to the maximum allowed λ, as introduced above, as well as using the notation of Tolhoek and Cox [21]. Among all parameters, the most frequently used are these with $\lambda = 1,2$, namely the first- and second-order orientation parameters, also known as *polarization* and *alignment*, respectively.

The polarization (also known as vector polarization [1]), i.e. the first-order orientation parameter f_1, is defined as an average value of the spin projection on the selected orientation axis (usually taken to be the z-axis) I_Z, normalized with the absolute spin value I [2]:

$$f_1(I) = \frac{\langle I_Z\rangle}{I} = \sum_m \left(\frac{m}{I}\right) p_m = -B_1(I)\sqrt{\frac{I+1}{3\,I}}. \tag{5}$$

The sign of polarization changes if the direction of the spins gets inverted.

Alignment (also known as tensor polarization [1]), i.e. the second-order orientation parameter f_2, on the other hand, quantifies the deviation from the uniform spin distribution towards a distribution favoring the spin projections along the z-axis:

$$\begin{aligned} f_2(I) &= \sum_m \left(\frac{m}{I}\right)^2 p_m - \frac{I+1}{3I} \\ &= B_2(I)\sqrt{\frac{(2I+3)(I+1)(2I-1)}{45\,I^3}}, \end{aligned} \tag{6}$$

where B_2 here is the nuclear orientation parameter B_{λ_j} for $\lambda_j = 2$. Alignment is a measure of the axially symmetric distribution of the spins, which means that the following is true: $p_m = p_{-m}$ (unlike for polarization where $p_m \neq p_{-m}$) [22]. Alignment is positive if the majority of spins are oriented along or against the z-axis, and negative if they are oriented perpendicular to it. The second-order parameter (as well as higher-order parameters with even values of λ) does not change in value if the direction of the nuclear spins is reversed.

The degree of polarization and alignment (i.e. f_1 and f_2) can be related to a given spin temperature β and be provided

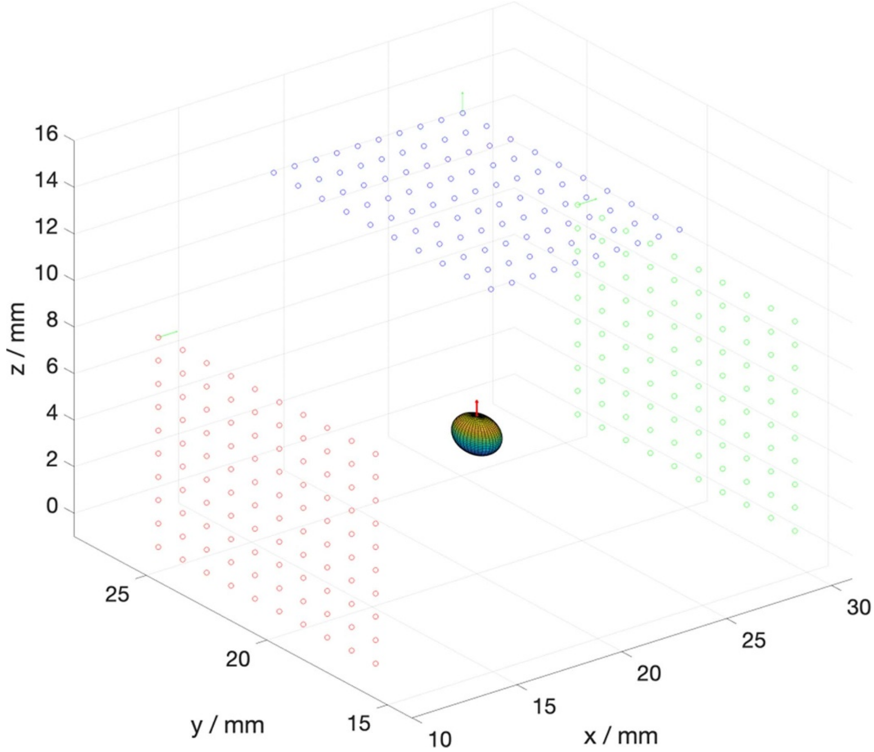

Figure 3. The first of two exemplary MATLAB simulation outputs of an ensemble of γ-ray emitting Xe nuclei emitted by a point-like source. Three detectors (green, blue, and red) with 10×10 sensors each are located around a sample of one voxel visualized with a red vector indicating its spin orientation and with a 3D surface plot indicating the directional distribution of emitted γ radiation. γ radiation is emitted isotropically from randomly oriented nuclei (no nuclear orientation: $\beta = 0, f_1 = 0$, and $f_2 = 0$), which is represented as a spherical 3D surface plot.

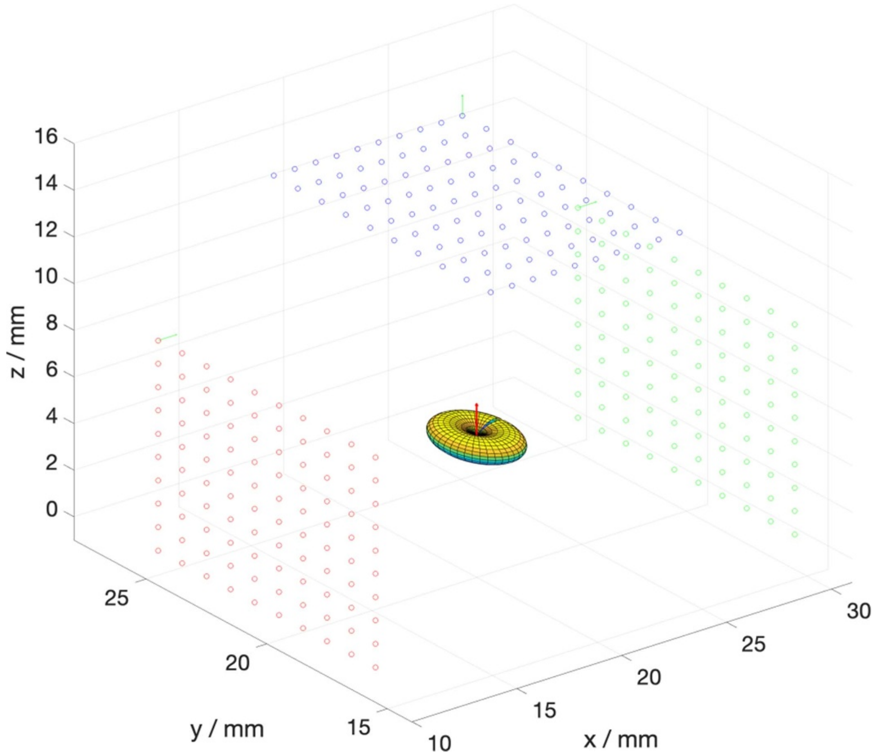

Figure 4. The second of two exemplary MATLAB simulation outputs of an ensemble of γ-ray emitting Xe nuclei emitted by a point-like source. Three detectors (green, blue, and red) with 10x10 sensors each are located around a sample of one voxel visualized with a red vector indicating its spin orientation and with a 3D surface plot indicating the directional distribution of emitted γ radiation. γ radiation is emitted anisotropically from (nearly) perfectly aligned spins ($\beta = 10, f_1 = 1$, and $f_2 = 0.606$), which is represented as an ellipsoidal 3D surface plot.

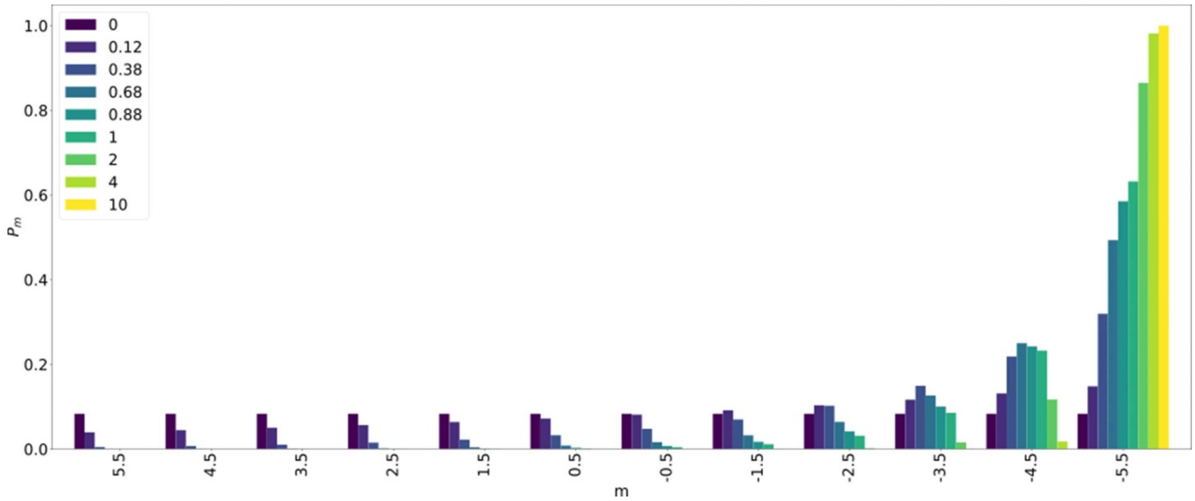

Figure 5. Population probability distributions p_m of magnetic sublevels m for mXe with $I_0 = {}^{11}/_2$ for selected values of spin temperature parameter β. Values of β are shown in the legend in the top-left corner.

as the output of the simulation together with the asymmetry in γ-ray emission.

2.4. Simulation of mXe γ-decay asymmetry detection for selected spin temperatures β

In the first step of the calculations outlined in previous subchapters, the coefficients A_λ and B_λ for mXe decay (with $I_0 = {}^{11}/_2$ and $\lambda = 2, 4, 6, 8$) were calculated for selected spin temperatures that represent an increasing degree of orientation. Next, they were used as input for MATLAB simulations of experimental γ-ray asymmetry for several detector geometries.

Figures 3 and 4 illustrate the geometry used in these simulations with three γ-ray detectors placed in two planes (blue in the $x-y$ plane; red and green in the $y-z$ plane), around an ensemble of γ-ray emitting xenon nuclei in a single voxel (i.e. a volume of space). The two panels represent the case of no nuclear alignment (a) and the case of perfectly aligned spins (b) along the external static magnetic field $\vec{\mathbf{B}}$ (z-axis), and thus emit γ-rays preferentially in the plane orthogonal to $\vec{\mathbf{B}}$.

The size of the detectors was set to $9 \times 9\,\mathrm{mm}^2$, while the source was assumed to be point-like, unless specified otherwise. The distance of the detectors to the source d_{sd} (set to be the same for three detectors) was a variable examined in this study, also represented as a solid angle Ω of γ-ray detection. The spherical and elliptical shapes of non-zero dimensions in figures 3 and 4 are the 3-dimensional reconstructions of the angular distribution of γ-ray emission from the source.

Given an equidistant placement of the γ-ray detectors from the point-like or finite-size unoriented source, the recorded count rate should be equal for all three detectors. In the case of nuclear alignment however, the γ-ray count rate increases for a detector placed transversely to $\vec{\mathbf{B}}$, and decreases for the detector placed longitudinally to $\vec{\mathbf{B}}$.

Let us consider an example for a point-like source of 30 MBq activity: with perfect detectors of the dimensions given above and placed at 20 mm from the source, one should expect to register $7.1 \cdot 10^5$ photon counts per second (cps) in all 3 detectors, if the sample is not oriented ($\beta = 0$), as shown in figure 3. For a (near) perfectly aligned sample ($\beta = 10$, shown in figure 4), one may expect $12.9 \cdot 10^5$ cps in the detector placed transversely to $\vec{\mathbf{B}}$, and $3.7 \cdot 10^5$ cps in the detector placed longitudinally to $\vec{\mathbf{B}}$. This is a significant change in the count rates of both detectors, which can be used as an efficient way of detecting the change in spin orientation, e.g. under rf excitations, as will be done in the GAMMA-MRI project.

3. Numerical results

Here, we present the magnetic substate populations for $^{129\mathrm{m},131\mathrm{m},133\mathrm{m}}$Xe at selected spin temperatures, and the resulting γ-ray counts registered in the detectors placed longitudinally and transversely to $\vec{\mathbf{B}}$ (at 0° and 90°).

3.1. Study cases

Figure 5 below presents magnetic sublevel population probabilities p_m for $^{129\mathrm{m},131\mathrm{m},133\mathrm{m}}$Xe corresponding to selected positive β values.

Although, unlike real temperature, T_s and β can be both positive and negative, because the angular distribution of gamma radiation is a function of even powers of m, it does not depend on the sign of T_s. Therefore, we have selected only positive β values.

Selected cases comprise:

- $\beta = 0$ resulting in isotropic γ-ray emission: $p_m = \frac{1}{12} = 0.083$ and all $B_\lambda = 0$;
- $\beta = 10$ giving extremely anisotropic γ-ray emission: $p(m = -11/2) = 0.99995$ (when $\beta \to \infty$, all populations are concentrated in $m_{\min}$: $p(m_{\min}) = 1$ and alignment is maximal: $f_2(\beta = 10) \approx f_2(\beta \to \infty) = 0.606$);
- Intermediate β values, including an example with $\beta = 0.38$, as discussed in [8].

Table 1. Nuclear orientation parameters f_1 and f_2 for studied spin temperature parameter β for mXe $\left(I_0 = {}^{11}/_2\right)$.

β	0	0.12	0.38	0.68	0.88	1	2	4	10
$f_1(I_0)$	0	−0.251	−0.630	−0.814	−0.871	−0.894	−0.972	−0.997	−1.000
$f_2(I_0)$	0	0.025	0.178	0.336	0.405	0.436	0.556	0.600	0.606
$\frac{f_1(I_0)}{f_{1\max}(I_0)}$ (%)	0	25	63	81	87	89	97	99.7	100
$\frac{f_2(I_0)}{f_{2\max}(I_0)}$ (%)	0	4	29	55	67	72	92	99	100

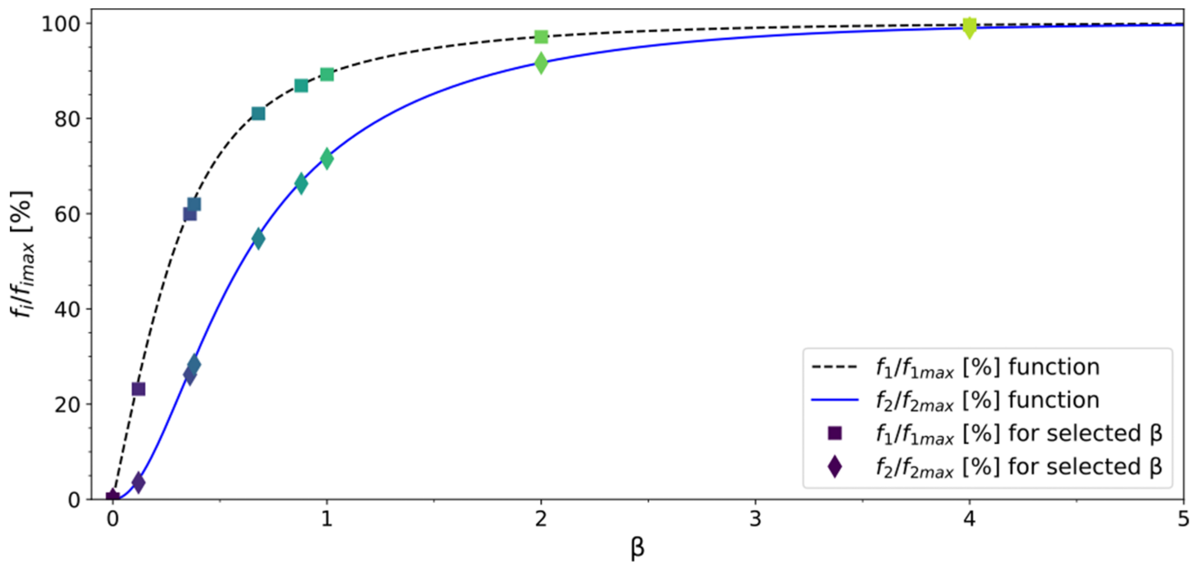

Figure 6. mXe spin polarization f_1 and spin alignment f_2 relative to their maximum values ($f_{1\max} = 1$ and $f_{2\max} = 0.606$) as a function of the spin temperature parameter β. $\beta = 10$ was used for normalization, as for this value, extremely high alignment and near-unity polarization are already achieved ($f_2(\beta \to \infty) \approx f_2(\beta = 10)$ and $f_1(\beta \to \infty) \approx f_1(\beta = 10)$).

Table 2. A_λ and $B_\lambda(\beta)$ coefficients for $M4$ γ-ray transition of $^{129\text{m},131\text{m},133\text{m}}$Xe from I $= {}^{11}/_2$ to I $= {}^{3}/_2$ for selected values of spin temperature parameter β.

λ	2	4	6	8
A_λ	0.89	0.44	0.03	0.26
$B_\lambda(\beta = 0)$	0	0	0	0
$B_\lambda(0.12)$	0.07	$\cdot 10^{-4}$	$\cdot 10^{-5}$	$\cdot 10^{-5}$
$B_\lambda(0.38)$	0.51	0.05	$\cdot 10^{-3}$	$\cdot 10^{-5}$
$B_\lambda(0.68)$	0.96	0.22	0.02	$\cdot 10^{-4}$
$B_\lambda(0.88)$	1.16	0.36	0.05	$\cdot 10^{-3}$
$B_\lambda(1)$	1.25	0.45	0.07	$\cdot 10^{-3}$
$B_\lambda(2)$	1.59	0.96	0.32	0.06
$B_\lambda(4)$	1.72	1.23	0.53	0.13
$B_\lambda(10)$	1.74	1.28	0.57	0.15

As detailed in table 1 and in the plot of $f_i(\beta)/f_i(\beta_{\max} = 10)$ (figure 6), analyzed β values span across the entire value range of the f_2 (and f_1) parameter. $\beta = 10$ is close to $\beta = \infty$ because in the latter case 99.95% of population is in the most extreme substate $m_{\min} = -I$ and alignment value f_2 is identical to 5 significant digits. Thus, $\beta = \infty$ was approximated by $\beta = 10$ in simulations while input $\beta = \infty$ was used for normalization.

Note that f_1 and f_2 are not mutually exclusive, and certain distributions of magnetic sublevels can be described simultaneously by non-zero values of polarization and alignment.

3.2. Numerical simulation of γ-ray angular distribution $W(\theta)$

For the study cases of mXe, the γ-ray multipolarity is $L = 4$ and thus $\lambda_{\max} = 8$. The angular distribution coefficients A_λ of this transition and the corresponding nuclear orientation coefficients B_λ for selected β values are listed in table 2.

Table 3. P_λ parameters for $M4$ transition $I = {}^{11}\!/_2$ to $I = {}^{3}\!/_2$ in ^{129m,131m,133m}Xe.

λ	$P_\lambda(\cos\theta)$
2	$\frac{1}{2}\left(3\cos^2\theta - 1\right)$
4	$\frac{1}{8}\left(35\cos^4\theta - 30\cos^2\theta + 3\right)$
6	$\frac{1}{16}\left(231\cos^6\theta - 315\cos^4\theta + 105\cos^2\theta - 5\right)$
8	$\frac{1}{128}\left(6435\cos^8\theta - 12012\cos^6\theta + 6930\cos^4\theta - 1260\cos^2\theta + 35\right)$

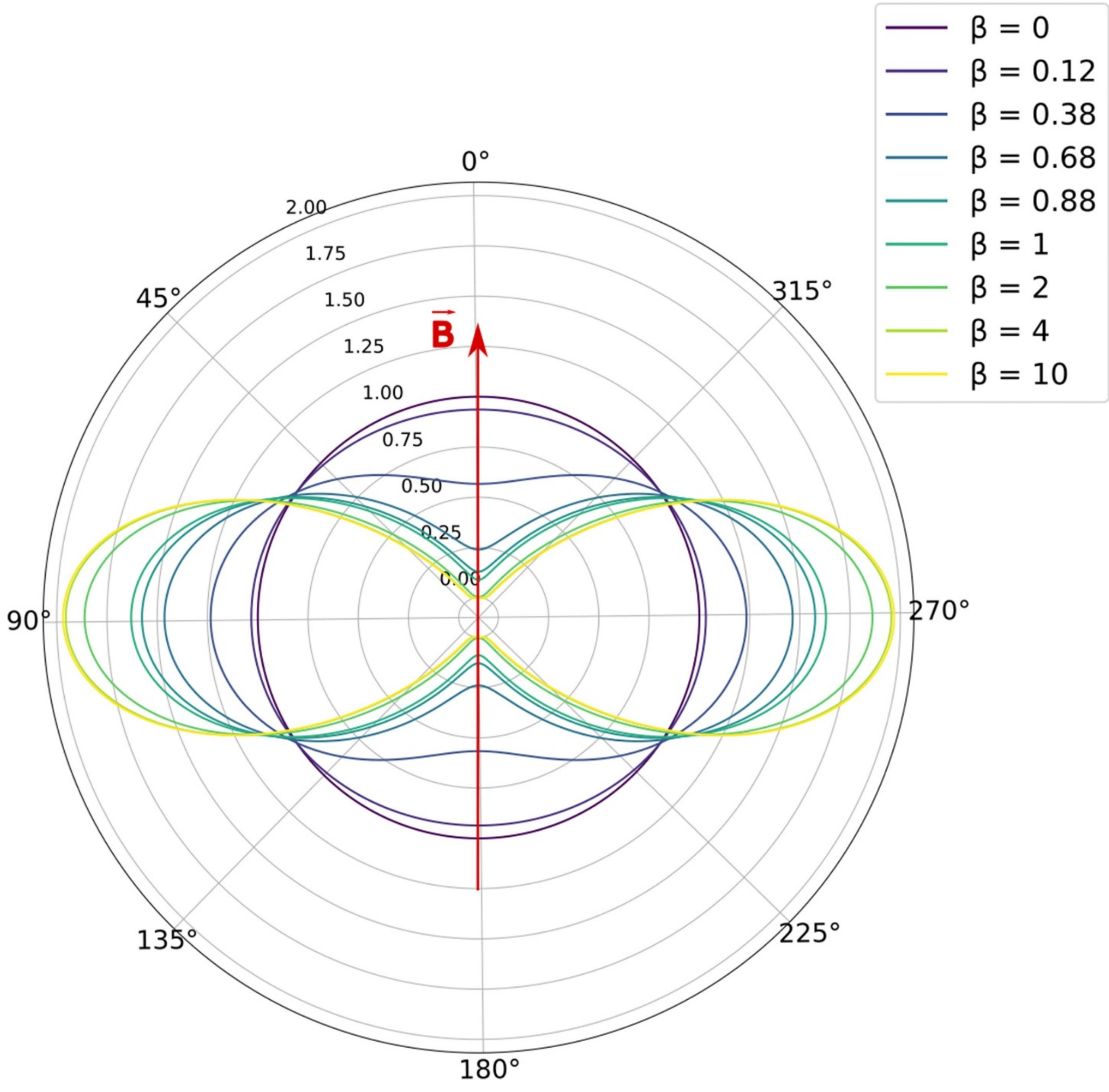

Figure 7. The angular distribution $W(\theta)$ of M4 γ radiation from mXe for the simulated cases of magnetic sublevel populations calculated using selected values of spin temperature parameter β. The direction of the external static magnetic field vector $\vec{\mathbf{B}}$ is marked in red. The extreme cases are marked in: purple (isotropic emission of γ radiation with $f_2 = 0$ for $\beta = 0$) and yellow (anisotropic emission of γ radiation with $f_{2\max} = 0.606$ for $\beta = 10$). The remaining plots represent $W(\theta)$ for the intermediate values of f_2 and β.

As mentioned in section 2.2, we take U_{λ_j}, G_λ, and Q_λ as each equal to 1. Thus, (4) takes the form:

$$W(\theta) = 1 + B_2A_2P_2(\cos\theta) + B_4A_4P_4(\cos\theta) + B_6A_6P_6(\cos\theta) + B_8A_8P_8(\cos\theta). \tag{7}$$

Legendre polynomials P_λ, using Rodrigues' formula, take the representation listed in table 3 for $\lambda = 2,4,6,8$. From table 2, one can see that as a general rule $B_2 > B_4 > B_6 > B_8$. Figure 7 presents the angular distribution of γ radiation for different β scenarios for mXe $\left(I = {}^{11}\!/_2\right)$.

The presented distributions are 2D cross-sections through 3D angular distributions along the $x-z$ plane (or $y-z$ plane due to the axial symmetry with respect to the x and y axes). Points at angles $\theta = 0°$ and $\theta = 180°$ lie in the axis of the

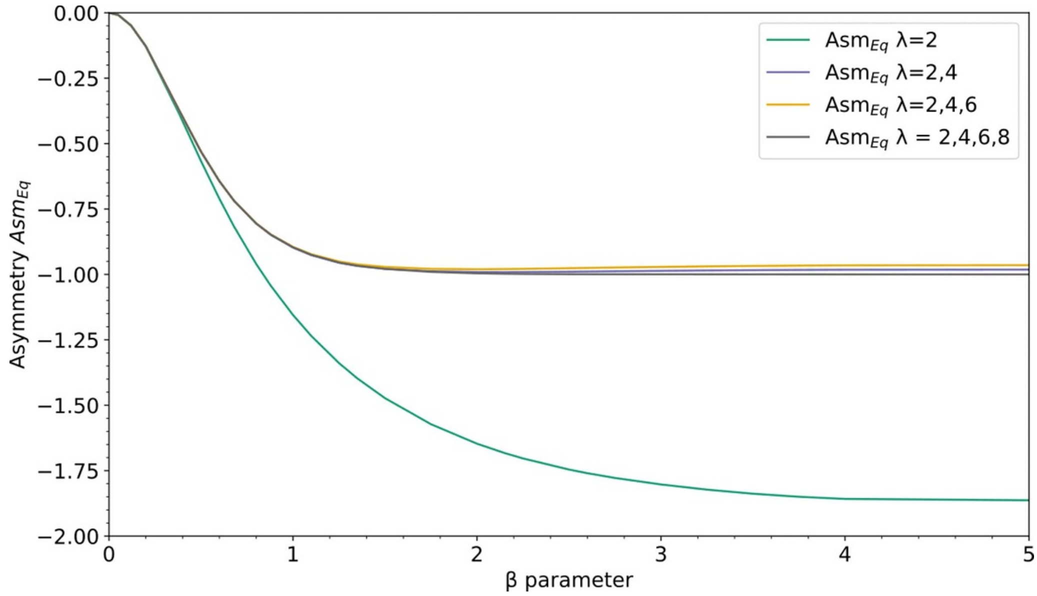

Figure 8. Analytical value of γ-ray asymmetry (between $\theta = 0^\circ$ and $\theta = 90^\circ$) emitted by mXe in the function of spin temperature parameter β. Four plots represent the expansion of $Asm_{Eq}\,(W(0), W(90)) = \frac{W(0)-W(90)}{W(0)+W(90)}$ formula to higher orders of λ: only $\lambda = 2$, $\lambda \in \{2,4\}$, $\lambda = \in \{2,4,6\}$, and all orders $\lambda = \in \{2,4,6,8\}$.

Table 4. Size of γ-ray source, distance and size of detectors, and observed asymmetry obtained with a MATLAB code relative to asymmetry for point-like source and detector.

Label	d_{sd} (mm)	Source (mm)	Solid angle Ω (%)	Asm/Asm_{eq}
Asm_{10s3}	10	3	—	0.9614
Asm_{10}	10	point-like	6.45	0.9834
Asm_{20}	20	point-like	1.61	0.9996
Asm_{50s20}	50	20	—	0.9995
Asm_{100}	100	point-like	0.01	1
Asm_{1000}	1000	point-like	$\cdot 10^{-4}$	1

magnetic induction vector $\vec{\mathbf{B}}$, denoted in red in figure 7. Along this axis, γ-ray emission decreases with an increasing degree of nuclear alignment (and spin temperature β). Points at angles $\theta = 90^\circ$ and $\theta = 270^\circ$ correspond to the plane orthogonal to the magnetic induction vector $\vec{\mathbf{B}}$. Along this plane, γ-ray emission increases with an increasing degree of nuclear alignment.

3.3. Simulation of γ-ray asymmetry observed with finite-size detectors

In this section, we look at the asymmetry of γ-ray detection, i.e. the difference in counts registered by finite-size detectors placed at $\theta = 0^\circ$ and $\theta = 90^\circ$ with respect to vector $\vec{\mathbf{B}}$. The detectors are placed around a point-like mXe source, all at the same distance d_{sd}.

Using (7), we first calculate the intensity of γ radiation for $\theta = 0^\circ$ and for $\theta = 90^\circ$, for which the biggest difference in the intensity of the emitted radiation is expected (see also figure 7 for the graphical representation of these equations):

$$W(0) = 1 + B_2A_2 + B_4A_4 + B_6A_6 + B_8A_8, \tag{8}$$

and:

$$W(90) = 1 - \frac{1}{2}B_2A_2 + \frac{3}{8}B_4A_4 - \frac{5}{16}B_6A_6 + \frac{35}{128}B_8A_8. \tag{9}$$

The resulting γ-ray asymmetry, i.e. relative difference in counts Asm_{Eq} at $\theta = 0^\circ$ and $\theta = 90^\circ$ angles, is given as:

$$Asm_{Eq}\,(W(0)\,, W(90)) = \frac{W(0) - W(90)}{W(0) + W(90)}$$
$$= \frac{192B_2A_2 + 80B_4A_4 + 168B_6A_6 + 93B_8A_8}{256 + 64B_2A_2 + 176B_4A_4 + 88B_6A_6 + 163B_8A_8} \tag{10}$$

The values of asymmetry from (10) calculated including only selected B_λ parameters are illustrated in figure 8 for the range of investigated $\beta \in \langle 0, 10\rangle$. From the figure, it is clear that one needs to include at least $\lambda = 2$ and $\lambda = 4$ to obtain an asymmetry that is close to the value including all four orders of B_λ. As the contribution from $\lambda = 6$ and $\lambda = 8$ is below 2% for $\beta > 2$, and even below 0.2% for $\beta \leqslant 1$, these two terms can be neglected in practical applications. Given that B_2 alone is not enough to describe accurately the decay asymmetry of mXe states, when discussing and interpreting γ-ray

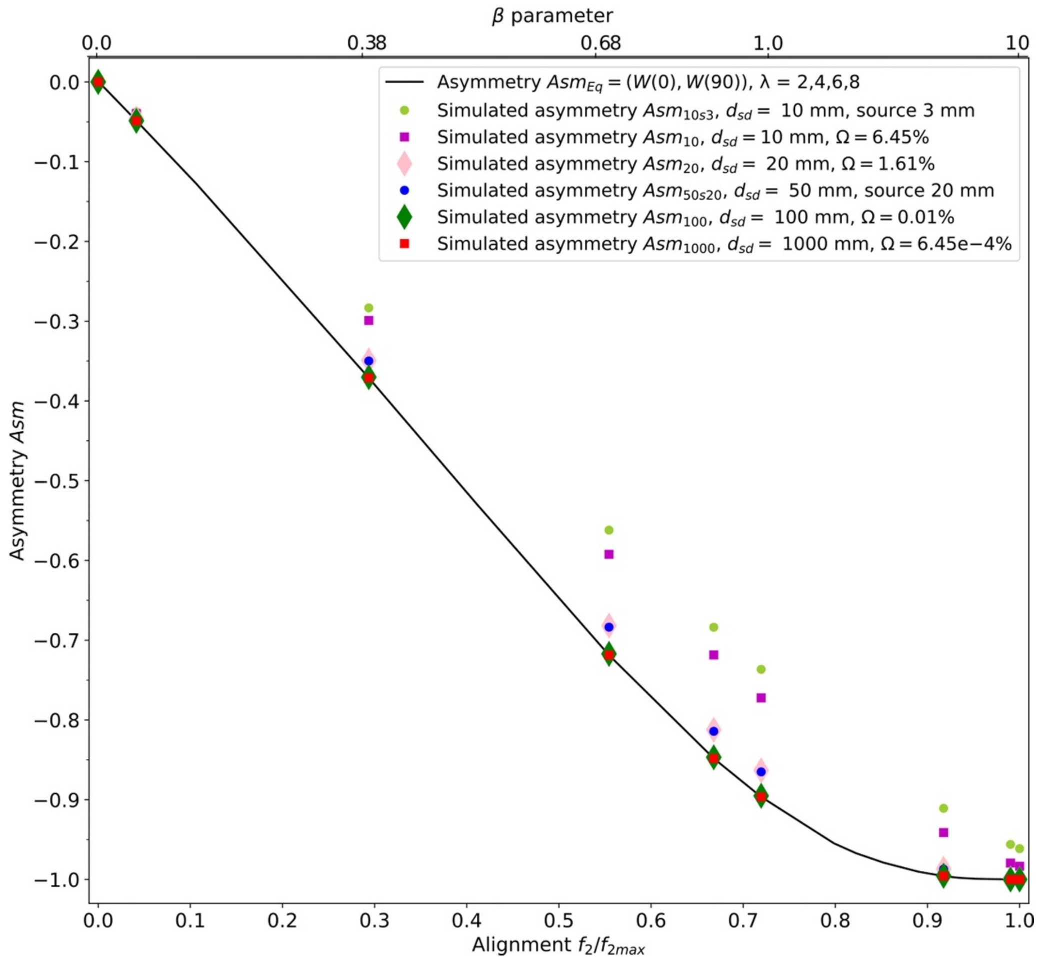

Figure 9. Simulated γ-decay asymmetry *Asm* for different source and detector sizes and distances d_{sd} as a function of spin temperature parameter β (top x-axis) and the corresponding relative alignment (bottom x-axis, $\frac{f_2}{f_{2\max}}$). For two datasets finite-size source was considered: 3 mm for Asm_{10s3} and 20 mm for Asm_{50s20}. For other datasets, a point-like source was assumed.

asymmetry, one should use both B_2 (alignment) and B_4 or spin temperature β (when the latter assumption can be considered to hold).

Using MATLAB simulations, we then studied the value of experimental asymmetry at selected β values for a point- or finite-size source, and finite-size detectors placed at varying distances d_{sd} representing different solid-angle coverage Ω, as summarized in table 4.

All datasets obtained from MATLAB simulations used detectors of size $9 \times 9\,\mathrm{mm}^2$, but a different distance d_{sd} from the source and various sizes of the source. One detector was located at $\theta = 0$, i.e. in the plane longitudinal to $\vec{\mathbf{B}}$ (blue detector in figures 3 and 4), while the second—at $\theta = 90$, in the plane transverse to $\vec{\mathbf{B}}$ (green or red detector in figures 3 and 4). All d_{sd} tabulated in table 4 were studied with point-like and finite-size sources, but for larger distances, $d_{sd} = 100\,\mathrm{mm}$ and $1000\,\mathrm{mm}$, no difference in *Asm* was observed. Thus, *Asm* values for finite-size sources are presented here only for smaller d_{sd}.

The values of Asm_{sd} for different d_{sd} in the function of spin temperature parameter β are represented with points in figure 9. For comparison, Asm_{Eq} for $\lambda = 2, 4, 6, 8$ is shown as a black line. All combinations of source and detector size, and distance, reach near-unity asymmetry at $\beta = 10$, except for $d_{sd} = 10\,\mathrm{mm}$. This is because in the latter case, the solid angle covered by one detector is no more negligible.

4. Conclusions and outlook

The purpose of this manuscript is to link the degree of nuclear orientation in metastable states of $^{129\mathrm{m},131\mathrm{m},133\mathrm{m}}$Xe isotopes of spin $I = {}^{11}\!/_2$ with the experimental asymmetry of their γ-ray emission. To this end, exact and approximate analytical equations, as well as numerical simulations were used to calculate the number of γ-rays reaching point-like and finite-size detectors placed at 0° and 90° to the spin direction. The study cases presented here correspond to the spin temperature parameter values $\beta \in \langle 0, 10 \rangle$, which is expected to describe the distribution of the magnetic sub-level population after Xe orientation with spin exchange optical pumping.

Nuclear orientation parameters f_1 and f_2, also known respectively as polarization and alignment, were also derived for each spin temperature value. These two parameters are commonly used to describe the nature and degree of spin orientation (it should be noted that they are not mutually exclusive and rather describe different orders/types of spin orientation). Although both are non-zero for most distributions of magnetic sublevels studied here, it is only the alignment that is relevant for the angular distribution of γ radiation. Furthermore, we saw that when assuming spin temperature, a relatively high polarization is accompanied by significantly lower relative alignment, except for high spin temperatures $\beta \geqslant 2$, where both parameters go over 90% of their maximal values. For instance, for $\beta = 0.38$ reached in [8] the degree of alignment corresponds to only 29% of its maximal value, while the polarization is already at 63%. Similar values were reached by [10].

Parameters A_λ, B_λ and Legendre polynomials $P_\lambda(\cos\theta)$ were then calculated to find the distribution of emitted γ radiation $W(\theta)$ and asymmetry $Asm(W(0), W(90))$. B_1 (proportional to spin polarization) and higher B_λ with odd λ do not appear in the equation for $W(\theta)$ in gamma decay, while even B_2 (spin alignment), B_4, B_6, and B_8 do. Their values for different β were calculated. Gamma decay asymmetry was then determined analytically for a point-like source and detectors, as well as using MATLAB simulations that included also finite sizes.

Next, the importance of higher-order orientation parameters B_λ was then studied. It was shown in particular that it is necessary to include B_4 parameter, while higher orders B_6 and B_8 can be fully neglected for spin temperature parameter $\beta < 1$, while giving a small, 2% correction for $\beta \geqslant 2$.

Furthermore, as expected, the smaller the solid angle covered by the detectors, the closer the asymmetry is to the idealized case of point-like detectors at 0° and 90° to the spin direction.

In the GAMMA-MRI project, a high degree of γ-decay asymmetry is desired. We have illustrated here that to achieve this goal, one ideally needs to reach with SEOP such a high spin temperature value that it corresponds not only to a high degree of polarization, but also that of alignment. In addition, the solid angle covered by the detectors should be as small as possible. Since the physical size of the detectors is a constraint, to increase the asymmetry, one can increase the distance to the source and/or use a small source. However, in the former case, the intrinsic detection probability of the γ-ray detectors and the activity of the γ-ray source have to be high enough to provide sufficient count rate statistics.

Recording angular γ-ray asymmetry is the basis for signal acquisition in the γ-ray detected MRI. For this reason, it was important to calculate the expected asymmetry for a range of experimental parameters, such as detector size and distance, and to test different analytical approximations. Such an analysis, presented in this manuscript, allowed us to determine that a high degree of spin polarization does not guarantee high alignment and high gamma-ray asymmetry. Also, certain approximations in the formula describing asymmetric decay are allowed. Finally, detector solid angles below 1% provide optimal geometries.

The above observations are of use for the GAMMA-MRI project, which aims to bring in a hybrid technique that combines the advantages of magnetic resonance imaging and nuclear medicine imaging.

The current proof-of-concept apparatus being built within that project provides the functionalities necessary for SEOP HP and γ-ray asymmetry acquisition. Funding was received from the European Union's Horizon 2020 research and innovation program under Grant Agreement No. 964644 (GAMMA-MRI) to finance the progress of the prospective setup. The next steps in the project cover, among others, realistic simulations, including biological modeling of the evolution of oriented mXe *in vivo* in the organ of interest, and the time dependence of the measured signal.

Data availability statement

The data cannot be made publicly available upon publication because they are not available in a format that is sufficiently accessible or reusable by other researchers. The data that support the findings of this study are available upon reasonable request from the authors.

Acknowledgments

The authors wish to thank Dr Jean-Noël Hyacinthe for early discussions and involvement in this project, and Ms Emma Wistrom for additional simulations at earlier stages of the project. The authors also wish to acknowledge support via the Swiss Excellence Government Scholarship (to K K), and via the CERN Medical Application Fund (GAMMA-MRI; to R B J and M K).

Conflict of interest

The authors declare that they have no known competing financial interests or personal relationships that could have appeared to influence the work reported in this paper.

ORCID iDs

Karolina Kulesz https://orcid.org/0000-0002-7108-0939
Robin Yoël Engel https://orcid.org/0000-0002-2347-241X
Renaud Blaise Jolivet https://orcid.org/0000-0002-5167-0851
Magdalena Kowalska https://orcid.org/0000-0002-2170-1717

References

[1] Niinikoski T O 2020 *The Physics of Polarized Targets* (Cambridge University Press)
[2] Postma H and Stone N J 1986 *Low-Temperature Nuclear Orientation* (North-Holland)
[3] Krane K S 1987 *Introductory Nuclear Physics* 3rd edn (Wiley)

[4] Biedenharn L C and Rose M E 1953 Theory of angular correlation of nuclear radiations *Rev. Mod. Phys.* **25** 729–77
[5] Feshbach H 1962 A unified theory of nuclear reactions. II *Ann. Phys., NY* **19** 287–313
[6] Rose M E 1953 The analysis of angular correlation and angular distribution data *Phys. Rev.* **91** 610–5
[7] Abragam A and Pound R V 1953 Influence of electric and magnetic fields on angular correlations *Phys. Rev.* **92** 943–62
[8] Calaprice F P, Happer W, Schreiber D F, Lowry M M, Miron E and Zeng X 1985 Nuclear alignment and magnetic moments of ^{133}Xe, ^{133}Xe^{m} and ^{131}Xe^{m} by spin exchange with optically pumped ^{87}Rb *Phys. Rev. Lett.* **54** 174–7
[9] Kitano M *et al* 1988 Nuclear orientation of radon isotopes by spin-exchange optical pumping *Phys. Rev. Lett.* **60** 2133–6
[10] Zheng Y, Miller G W, Tobias W A and Cates G D 2016 A method for imaging and spectroscopy using γ-rays and magnetic resonance *Nature* **537** 652–5
[11] Yoel Engel R 2018 Master Thesis *Planing, simulation and preparation of a magnetic resonant imaging experiment based on the detection of anisotropic gamma-radiation from hyperpolarized isomers* (Oldenburg University) (available at: https://cds.cern.ch/record/2638538)
[12] Walker T G and Happer W 1997 Spin-exchange optical pumping of noble-gas nuclei *Rev. Mod. Phys.* **69** 629–42
[13] Stupic K F, Cleveland Z I, Pavlovskaya G E and Meersmann T 2011 Hyperpolarized ^{131}Xe NMR spectroscopy *J. Magn. Reson.* **208** 58–69
[14] Norquay G, Collier G J, Rao M, Stewart N J and Wild J M 2018 ^{129}Xe–Rb spin-exchange optical pumping with high photon efficiency *Phys. Rev. Lett.* **121** 153201
[15] Nikolaou P *et al* 2013 Near-unity nuclear polarization with an open-source ^{129}Xe hyperpolarizer for NMR and MRI *Proc. Natl Acad. Sci. USA* **110** 14150–5
[16] Abragam A and Proctor W G 1958 Spin temperature *Phys. Rev.* **109** 1441–58
[17] Timar J, Elekes Z and Singh B 2014 Nuclear data sheets for A = 129 *Nucl. Data Sheets* **121** 143–394
[18] Khazov Y, Mitropolsky I and Rodionov A 2006 Nuclear data sheets for A = 131 *Nucl. Data Sheets* **107** 2715–930
[19] Khazov Y, Rodionov A and Kondev F G 2011 Nuclear data sheets for A = 133 *Nucl. Data Sheets* **112** 855–1113
[20] Alder K and Winter A 1975 *Electromagnetic Excitation* (North-Holland)
[21] Tolhoek H A and Cox J A M 1952 Angular distribution and polarization of gamma radiation emitted by aligned radioactive nuclei *Physica* **18** 357–8
[22] Neyens G 2003 Nuclear magnetic and quadrupole moments for nuclear structure research on exotic nuclei *Rep. Prog. Phys.* **66** 1251